Bistatic electromagnetic scattering by sea surface using two-scale model with Elfouhaily spectrum

M.Y. Ayari, A. Khenchaf, A. Coatanhay

Laboratoire E^3I^2, ENSIETA, 2 rue François verny 29806 Brest cedex 9 France, {yassinmo, khenchal, coatan}@ensieta.fr

Abstract: Electromagnetic scattering by sea surface is estimated using most common approaches for scattering by rough surfaces, and different sea wave models are compared. After a brief presentation of these models and approaches, this study points out the Elfouhaily surface model. Finally, both monostatic and bistatic configurations are treated using-two scale model.

Keywords: electromagnetic bistatic scattering, random rough surfaces, sea spectrum.

1. Introduction

To describe random sea surface, several mathematical statistical models were developed. Some based on surface spectrum and others on slope distributions depending on the surface roughness.

Gaussian models were the first and simplest ones to depict surface random behaviour; they were widely used in literature. Two parameters had to be fixed, variance and correlation distance in spectrum definition and slopes variances up and cross the wind direction for the slopes distribution model. These classical models were rejected since they do not reproduce the real phenomena.

Using wave recording systems (aircraft, pressure transducer, NIO pitch-roll buoy), new theories and models of sea wave appeared. Cox and Munk [3] came up with a practical statistical expression of sea slopes. Their work was based on sun Glitter sea surface photographs. They treated two types of surfaces with different wind velocities: slick and clean sea. The first model is a surface covered with a thin oil layer to attenuate the capillarity waves. These later will be present in the second model whereas the gravity waves were omitted.

Several spectrum definitions were developed for sea surface interpretation. In this paper, we limit to two spectrum models: Pierson Moskowitz [5] adapted by Fung and Lee [4], and Elfouhaily and al [2]. The former is a band-defined expression depending in the wave nature (capillary or gravity waves). The later is expressed as a sum of two spectrum regimes (low and high frequency).

These surface definitions are used to estimate the electromagnetic sea scattering. Different approaches have been developed for this issue; each of them is appropriated to given sea wave conditions. When surface roughness level is much greater than the transmitted wavelength, Kirchhoff approximation is the finest approach to model the scattering phenomenon. The small perturbation model is dedicated to the computation of the contribution of roughness scale much smaller than wavelength. To overcome the restricted validity of the both former classical analytic approaches, an efficient two-scale model [1] is employed.

The first part of this paper deals with sea surface models developed in the literature. A comparison between classical approaches and our two scale model is presented at the end of this section. Next, three approaches of scattering estimation will be discussed. A validation step will be completed by a comparison with literature in backscattering configuration. The last section will be devoted to electromagnetic bistatic simulation using two-scale approach, Pierson-Moskowitz and Elfouhaily spectrum.

2. Sea surface models

At each point of the sea surface, waves result from a sum of waves locally generated by wind and waves coming from any other areas. Due to these interactions, the phenomenon can hardly be quantified. Since the ocean presents an uncoordinated aspect, the sea fluctuations are classically represented by three dimensional random process $z(\vec{r}, t)$ one temporal and two spatial components. The vector $\vec{r}$ (x, y) stands for the spatial location of the point represented by its cartesian coordinates *(x, y, z)* at the time *t*. During this work we omit the time component. The process is supposed to be stationary and ergodic. In this case, the surface behaviour can completely be determined by the knowledge of its spectrum and its slope density probability.

2.1 Sea slope distribution

As far as slopes are randomly distributed, the first form to define sea slopes density probability was the Gaussian distribution. It can take into account the wind speed effect. However, this function is symmetric with the up wind direction. This property is not consistent with the physical sense and actual data.

Cox and Munk studied the slopes distributions of smaller waves on the sea surface; they get measures from an aircraft by means of photographs of the glitter pattern. Lines with equal glitter intensity represent points on the sea surface where the slope reflects the sun to the camera. Their theory and results both show that the number of glitter points was the greatest at the specular point and

that the probability density function for this glitter was nearly bivariate normal with the variances in the upwind direction being larger than the variances in the crosswind direction. They also underlined the asymmetry of the upwind density function, a property that wasn't respected in the previous model. These observations were interpreted in their slopes probability distribution.

2.2 Sea spectrum

During the 60's, sea spectra have been studied at various frequencies band (L to K_u). Classically, a sea spectrum is set to

$$S(k,\phi) = M(k) f(k,\phi) \quad [1]$$

Where $M(K)$ represents the isotropic part of the spectrum modulated by the angular function $f(K, \phi)$. K and ϕ are respectively the spatial wave number and the wind direction. In this section we will give hints of models from literature: Pierson-Moskowitz and Elfouhaily.

Pierson-Moskowitz model:

The semi-empirical sea spectrum presented in this section is based upon studies by Pierson and Pierson-Moskowitz. They defined a band spectrum depending on the wave's nature (capillary or gravity wave). Fung and Lee introduced little changes to answer the continuity properties. The spectrum form is then given by

$$S(K) = \begin{cases} S_1(K), & K < K_j \\ S_2(K), & K \geq K_j \end{cases} \quad [2]$$

where K_j=0.04 rad/cm (so that $S_1(K_j)=S_2(K_j)$)

To account for the anisotropic effect due to wind direction, Pierson come up with the angular function $f(\phi)$, (ϕ is the wind direction), it was adopted by Fung to $f(K, \phi)$ [4] and given by

$$f(K,\phi) = a_0 + a_1\left(1 - e^{-bK^2}\right)\cos 2\phi \quad [3]$$

where $a_0 = (2\pi)^{-1}$, $b \approx 1.5\,\mathrm{cm}^2$, $a_1 = \dfrac{1-R}{1+R}$ and $R = \dfrac{0.003 + 1.92\times10^{-3} U_{12.5}}{3.16\times10^{-3} U_{12.5}}$, ($U_{12.5}$: wind speed at an altitude of 12.5 meters above the sea surface)

Elfouhaily model:

It was introduced in 1997 and was also called unified spectrum. Its objectives were to reproduce certain observations such as those inferred by Cox and Munk and introduce the wave age dependency (fetch). The spectrum definition is much more tractable than the previous one. The analytic expression is available for all the wave number bands. It is a sum of two components capillary and gravity, each of then is dominant when situated in its band. The whole sea wave spectrum is then timed by a common term.

$$S(K) = \left(S_c(K) + S_g(K)\right) S_{com}(K) \quad [4]$$

Indexes c and g correspond to the capillarity and gravity waves. To cover the bidimentional domain, the unified spreading function was defined as follows:

$$f(K,\phi) = \frac{1}{2\pi}\left[1 + \Delta(K)\cos(2\phi)\right] \quad [6]$$

This function is centrosymmetric as required by Guissard [11]work. $\Delta(K)$ is recognized as the coefficient of the second harmonic when truncating the Fourier series expansion of $f(K, \phi)$.

Sea models seen in this section will be widely used in RCS valuation.

3. Bistatic scattering coefficient estimation

Many approaches were developed to evaluate the electromagnetic sea surface scattering; each is available in certain hypothesis and conditions. In this paper, we present three models: Kirchhoff approximation, small-perturbation model and a two-scale model. The geometry of the surface scattering reflection is shown in figure 1

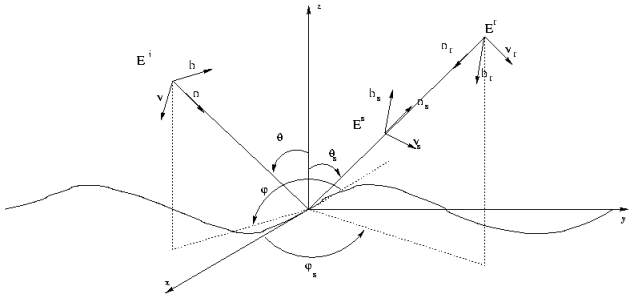

Figure 1 : Geometry of a surface bistatic scattering problem

3.1 Kirchhoff approximation

The vector formulation of the Kirchhoff method is based on the vector second Green theorem, which states that the scattered field at any point within the source-free region bounded by a closed surface can be expressed in terms of the tangential fields to the surface. A mathematical statement of this is as follows

$$\vec{E}_s = -jk\frac{e^{-jkR_0}}{4\pi R_0}\vec{n}_s \wedge \int [\vec{n} \wedge \vec{E} - \eta_s \vec{n}_s \wedge (\vec{n} \wedge \vec{H})] e^{jk\vec{r}\cdot\vec{n}_s} ds \quad [6]$$

where $\vec{n}_s$ is the unit vector in the scattered direction, $\vec{n}$ is the unit vector normal to the surface, $\eta_s = \sqrt{\mu/\varepsilon}$ is the intrinsic impedance of the medium, R_0 is the distance from the center of illuminated area to the point of observation, $\vec{E}$ is the total electric filed and $\vec{H}$ is the magnetic field.

Kirchhoff approximation is valid when the surface with horizontal roughness scale and average radius of curvature are larger than the electromagnetic wavelength (kL>6 and R_c>λ, where L states for the surface correlation length, and R_c is the average radius of curvature for the rough surface). In other word, this method is valid for the specular field component. When both the surface standard deviation and the correlation length are smaller than the wavelength, another standard approach is considered: the small perturbation model.

3.2 Small-perturbation model

This model was introduced by Rice. Starting from the Maxwell equations and using the electromagnetic field expression combined with the reflectivity coefficient, a

six differential equation system is generated. Using the first order Fourier development, the system is then simplified to a linear one. This is possible when the surface irregularities are small within the electromagnetic wavelength. The bistatic scattering coefficient for either horizontally or vertically polarized incident wave is

$$\sigma_{pq}^{s} = 8\left|k^2 \cos\theta \cos\theta_s \alpha_{pq}\right|^2 S\left(k_x + k\sin\theta, k_y\right) \qquad [7]$$

where $\begin{cases} k_x = -k\sin\theta_s \cos\varphi_s \\ k_y = -k\sin\theta_s \sin\varphi_s \\ k_z^2 = k^2 - k_x^2 - k_y^2 \end{cases}$

and S is the surface spectrum and α_{pq} [1] is defined with the incident and received polarisation (horizontal or vertical). Unlike the previous model, small perturbation model is not appropriate for the specular component. In return, the small perturbation method is very reliable when estimating scattered electromagnetic fields. For grazing angles neither Kirchhoff method nor small perturbation model is able to valuate the electromagnetic field. To solve this problem we use the two-scale model.

3.3 Two-scale model

In reasonable way, ocean surfaces roughness can be split into two scales: a large and small with the incident electromagnetic wave. The previous approaches are available for particular surface degrees. Two-scale approach cover a larger domain, it is commonly used in the recent literature [1].

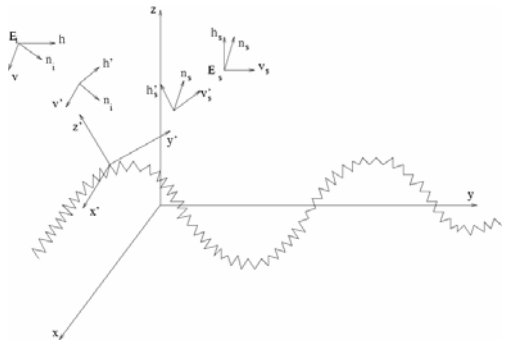

Figure 2 : Geometry of a surface bistatic scattering in the two-scale model

The main idea of this method is to take advantages of the two previous approaches and enlarge the application domain. In this case, the surface spectra of large-scale waves and small-scale waves, denoted by S_l and S_s, respectively, are related to the sea surface spectrum S by

$$S_l(K,\phi_k) = \begin{cases} S_l(K,\phi_k) & \text{if } K < k_d \\ 0 & \text{otherwise} \end{cases} \qquad [8]$$

$$S_s(K,\phi_k) = \begin{cases} 0 & \text{if } K < k_d \\ S_s(K,\phi_k) & \text{otherwise} \end{cases} \qquad [9]$$

where k_d is the two-scale cutoff, it is estimated to $k/3$ [7]. When located in the gravity domain ($K < k_d$), the electromagnetic scattering wave is estimated by Kirchhoff approximation. In the capillary region, the RCS is evaluated using an adapted small perturbation model. It is leading idea to focalise on the local reference of the incident wave and use the classical small perturbation approach. The result is then adapted to the real surface by a tilting process. This is necessary to average the σ_{pq}, see eq.[7], over the slope distribution (as viewed by the receiver) for the large-scale waves. The scattering matrix [S] is given by [1] [12]

$$[S] = \begin{bmatrix} v'_s \cdot v_s & h'_s \cdot v_s \\ v'_s \cdot h_s & h'_s \cdot h_s \end{bmatrix} \begin{bmatrix} S_{v'_s \cdot v'} & S_{v'_s \cdot h'} \\ S_{h'_s \cdot v'} & S_{h'_s \cdot h'} \end{bmatrix} \begin{bmatrix} v' \cdot v & v' \cdot h \\ h' \cdot v & h' \cdot h \end{bmatrix} = \begin{bmatrix} \sigma_{vv}^s & \sigma_{vh}^s \\ \sigma_{hv}^s & \sigma_{hh}^s \end{bmatrix} \qquad [8]$$

where

$$\begin{aligned} \sigma_{pq}^s = &< (p.v'_s)^2 (q.v')^2 \sigma_{v'_s v'} + (p.v'_s)^2 (q.h')^2 \sigma_{v'_s h'} + (p.h'_s)^2 (q.v')^2 \sigma_{h'_s v'} \\ &+ (p.h'_s)^2 (q.h')^2 \sigma_{h'_s h'} + (p.h'_s)^2 (q.v')(q.h') \sigma^1_{h'_s h' h'_s v'} \\ &+ (p.v'_s)(p.h'_s)(q.h')^2 \sigma^1_{h'_s h' v'_s h'} + (p.v'_s)(p.h'_s)(q.h')(q.v') \sigma^1_{h'_s v' v'_s h'} \\ &+ (p.v'_s)(p.h'_s)(q.v')^2 \sigma^1_{h'_s v' v'_s v'} + (p.h'_s)^2 (q.v')(q.h') \sigma^1_{v'_s v' v'_s h'} > \end{aligned} \qquad [9]$$

$$\sigma^1_{pqp'q'} = 16\left|k^2 \cos\theta' \cos\theta'_s\right|^2 \mathrm{Re}\left(\alpha_{pq} \alpha^*_{pq}\right) S\left(k_x + k\sin\theta, k_y\right) \qquad [10]$$

and σ_{pq} is given by eq.[7]

θ' is the local incidence angle, θ'_s is the local scattering angle.

Two-scale model has a larger domain than the Kirchhoff and the small perturbation approaches. It covers the small and the large waves. If compared to the classical models, our two scale approach is far more reliable to estimate the specular electromagnetic fields as well as the scattered one especially for the grazing angles.

4. Numerical analysis

Before simulating scattering coefficients in bistatic configuration, a comparison with literature is necessary to validate our model. In this part, the first part of this section treats backscattering configuration. The bistatic case is represented at the end of this section.

4.1 Backscattering configuration

This configuration is omnipresent in the literature, it is simple to implement since the emitter is in the same time the receiver. It is used in many applications as classic radars, SAR images and GBR…

To fulfil the backscattering configuration conditions, incident angles in emission and reception must be identical and the corresponding azimuth difference equal to π.

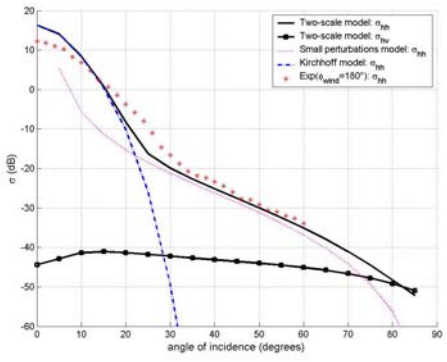

Figure 3(a) : Backscattering coefficients (different models) (F=14 GHz, T=20°C, S=35ppt, wind speed=5 m/s (at 10 m)) (Two-scale model, Small perturbations model, Kirchhoff model are compared with Voronovitch experimental data [9])

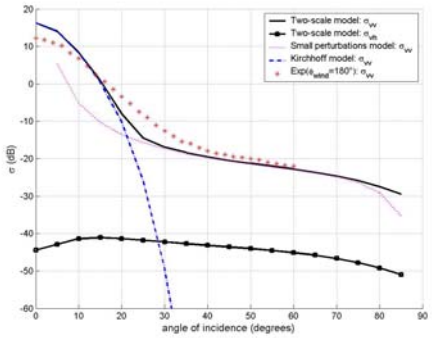

Figure 3(b) : Backscattering coefficients (different models) (F=14 GHz, T=20°C, S=35ppt, wind speed=5 m/s (at 10 m)) (Two-scale model, Small perturbations model, Kirchhoff model are compared with Voronovitch experimental data [9])

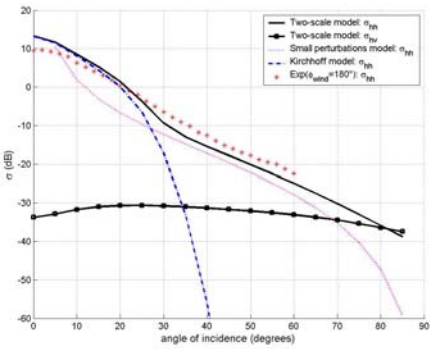

Figure 4(a) : Backscattering coefficients (different models) (F=14 GHz, T=20°C, S=35ppt, wind speed=15 m/s (at 10 m)) (Two-scale model, Small perturbations model, Kirchhoff model are compared with Voronovitch experimental data [9])

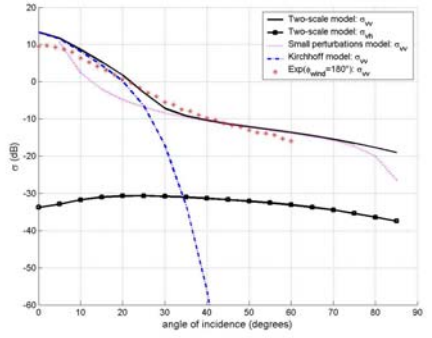

Figure 4(b) : Backscattering coefficients (different models) (F=14 GHz, T=20°C, S=35ppt, wind speed=15 m/s (at 10 m)) (Two-scale model, Small perturbations model, Kirchhoff model are compared with Voronovitch experimental data [9])

In examining the data points shown in figures 3 (a,b) and 4 (a,b), several items of importance may be deduced from the graphs. First, there is rather a good agreement between the calculated cross sections and the ocean measurements depending on the used approach and sea representation. Near the normal (specular region in backscattering configuration $0<\theta=\theta_s<20°$) Kirchhoff is fitted to the data.

This statement constitutes a logical consequence since this configuration really fulfils the Kirchhoff validity conditions.

In the median region ($25°< \theta=\theta_s <60°$) Small perturbations model is the adequate approach for this domain as well as the two-scale one. In this case waves are relatively small compared to the spatial wave number. For the grazing angles ($\theta=\theta_s >60°$) neither the Kirchhoff method nor the Small perturbations model are adapted to determine the scattering matrix coefficients. However two-scale approach gives credible results. Indeed when focusing in the local reference we can use small perturbation model since we respect its hypothesis, the averaging result by the slope distribution (tilting process) will adapt the results to the global reference so come the importance of this approach. Finally we underline the performances of the two-scale approach in evaluating the cross coefficients evaluation σ_{hv} and σ_{vh} that they are estimated null by the other models.

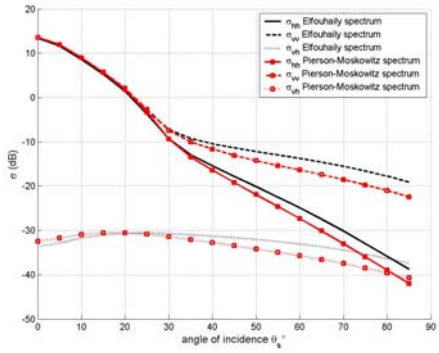

Figure 5 : Back scattering coefficients (with different sea spectrums and using two-scale model) (F=14 GHz, T=20°C, S=35ppt, wind speed=15 m/s (at 10 m)

In the same way, from figure 5 we may evaluate the different sea surface representation through their impact on the scattering coefficients. The results point out a difference of 0 to 5 (dB) between the two sea spectra using two-scale model.

Figures 6 (a,b) reveal that electromagnetic coefficients reach their maximum for both upwind and downwind direction and their minimum at the cross wind direction. Two-scale and small perturbation models confirmed their validity for the intermediate domain since results are in good agreement with Moore and Fung data for an incident angle of 40°. Yet Kirchhoff approach is not exploitable in this case: we are far from the specular region.

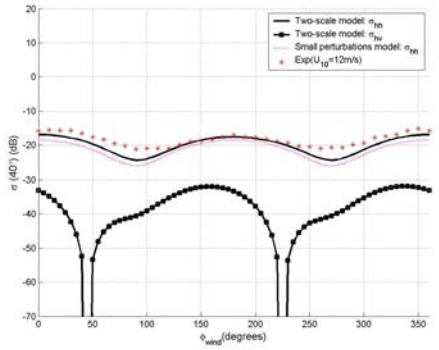

Figure 6(a) : Back scattering coefficients (diffrent models) (F=14 GHz, T=20°C, S=35ppt, wind speed=12 m/s (at 10 m), $\theta=\theta_s=40°$) (Two-scale model, Small perturbations model, Kirchhoff model are compared with Moore and Fung experimental data [10])

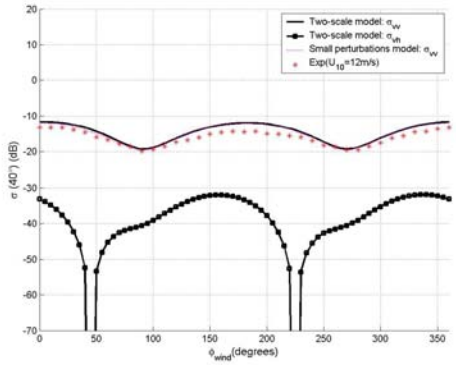

b

Figure 6(b) : Back scattering coefficients (diffrent models) (F=14 GHz, T=20°C, S=35ppt, wind speed=12 m/s (at 10 m), $\theta=\theta_s=40°$) (Two-scale model, Small perturbations model, Kirchhoff model are compared with Moore and Fung experimental data [10])

4.2 Bistatic configuration

Most of the bistatic simulations illustrated in the literature treat either the forward or backward scattering. We represent both of these configurations in the same graph. Then incident angle in the emission θ is fixed (60° and 80°) while the received one θ_s varies from -90° to 90°. Received azimuth φ_s is set to 0°.

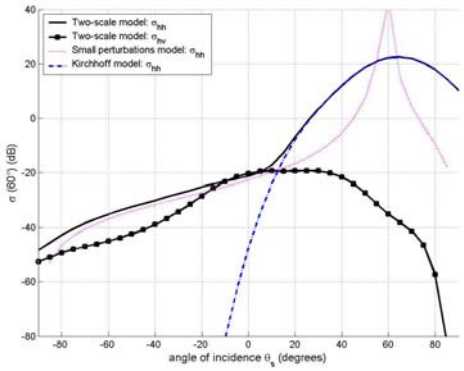

Figure 7(a) :Scattering coefficients (bistatic configuration) F=14 GHz, T=20°C, S=35ppt, wind speed=5 m/s (at 10 m) φ_s=180°, θ=60° (Two-scale model, Small perturbations model, Kirchhoff approach)

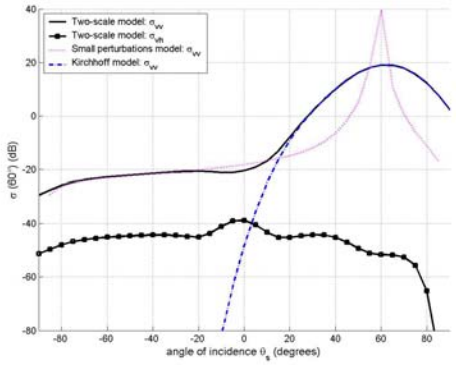

Figure 7(b) :Scattering coefficients (bistatic configuration) F=14 GHz, T=20°C, S=35ppt, wind speed=5 m/s (at 10 m) φ_s=180°, θ=60° (Two-scale model, Small perturbations model, Kirchhoff approach)

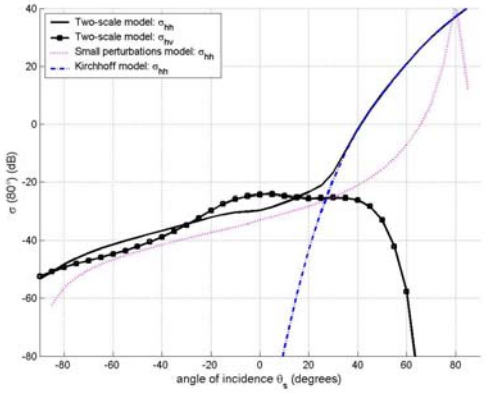

Figure 8(a) :Scattering coefficients (bistatic configuration) F=14 GHz, T=20°C, S=35ppt, wind speed=5 m/s (at 10 m) φ_s=180°, θ=80° (Two-scale model, Small perturbations model, Kirchhoff approach)

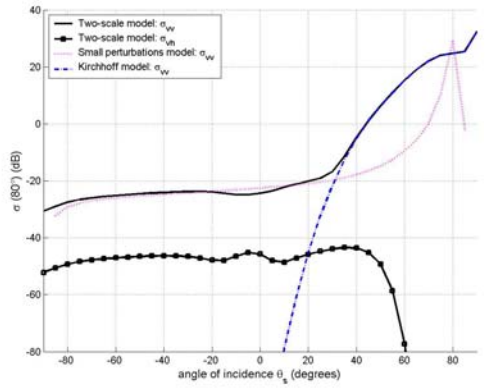

Figure 8(b) :Scattering coefficients (bistatic configuration) F=14 GHz, T=20°C, S=35ppt, wind speed=5 m/s (at 10 m) φ_s=180°, θ=80° (Two-scale model, Small perturbations model, Kirchhoff approach)

In the last simulation figure 9, all the previous conditions are the same but the receiver azimuth φ_s is set to 90°. More, only the two-scale approach is investigated.

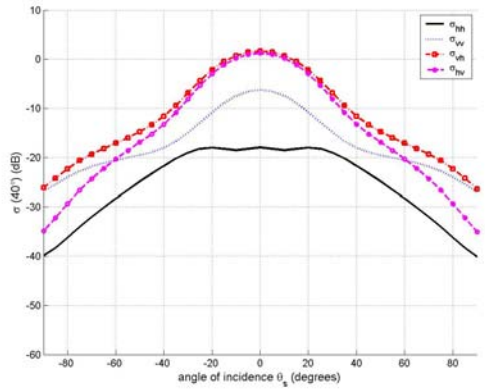

Figure 9(a) :Scattering coefficients (bistatic configuration) F=14 GHz, T=20°C, S=35ppt, wind speed=5 m/s (at 10 m) φ_s=90°, θ=60° (Two-scale model, Small perturbations model, Kirchhoff approach)

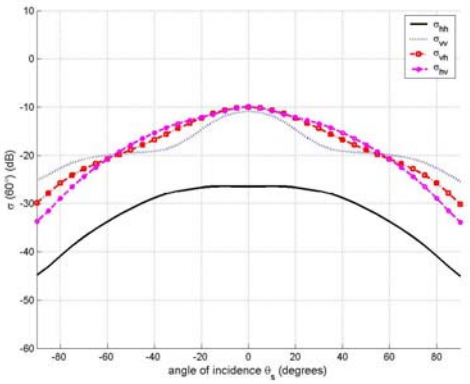

Figure 9(b) :Scattering coefficients (bistatic configuration)
F=14 GHz, T=20°C, S=35ppt, wind speed=5 m/s (at 10 m) φ_s=90°, θ=60° (Two-scale model, Small perturbations model, Kirchhoff approach)

Conclusion

For sea surface, the two-scale model describing bistatic reflectivity was presented. Using the Semi-empirical and unified spectrum, numerical results were computed for the bistatic radar cross section from, related to physical parameters (wind direction and velocity, water salinity and temperature, frequency). Actually we are carrying out a comparison of Voronovitch model with the two-scale in bistatic configuration.

Bibliography

[1] A. Khenchaf: "*Bistatic radar moving returns from sea surface*", IEICE Trans. Elct., E83-C, 1827-1835, 2000.

[2] T. Elfouhaily, B. Charpon, K. Katsaros: "*A unified directional spectrum for long and short wind-driven waves*", IEEE, 102, 15781-15796, 1997.

[3] C. S. Cox, W. H. Munk: "*Statistics of the sea surface derived from sun glitter*", J. Mar. Res, 13, 198-226, 1958.

[4] A. K. Fung, K. K. Lee: "*A semi-empirical sea-spectrum model for scattering coefficient estimation*", IEEE Jou. Ocean. Engine, OE-7 No 4, 166-176, 1982.

[5] W. J. Pierson: "*A semi-empirical sea-spectrum model for scattering coefficient estimation*", NASA contract report, CR-2646n, N76-17775, 1991.

[6] G. Soriano and M. Saillard: "*Modelization of the scattering electromagnetic waves from the ocean surface*", PIER, 37, 101-128, 2002.

[7] J. T. Johnson, R. T. Shin, J. A. Kong, L. Tsang and K. Pak "*A numerical study of the composite surface model for ocean backscattering*" IEEE Trans. Geosci. Remote Sensing, 36, 72-83, 1998.

[8] A. K. Fung, C. Zuffada, and C. Y. Hsieh "*Incoherent Bistatic Scattering from the Sea Surface at L-Band*" IEEE Trans. Geosci. Remote Sensing, 39, No5, 1049-1060, 2001

[9] A. G. Voronovitch and V. U. Zavorotny "*Theoretical model for scattering of radar signals in K_u and C-bands form a rough sea surface with breaking waves*". Wave in Random Media, 11, 247-269 (2001)

[10] R. K. Moore and A. K. Fung "*Radar determination of winds at sea*" IEEE, 67, No11, 1504-1521, 1979

[11] A. Guissard "*Directional spectrum of the sea surface and wind scatterometry*" Int. J. Remote Sens., 14(8), 1615-1633, 1993

[12] A. Khenchaf "*Bistatic scattering and depolarization by randomly rough surfaces: application to the natural rough surfaces in X-band*" Waves in Random Media 11, 61-89, 2001